

Influence of Processing Conditions and Physicochemical Interactions on Morphology and Fracture Behavior of a Clay/Thermoplastic/Thermosetting Ternary Blend

M. Hernandez,^{1,2,3} J. Duchet-Rumeau,^{1,2,3} H. Sautereau^{1,2,3}

¹Université de Lyon, Lyon F-69003, France

²INSA Lyon, Villeurbanne F-69621, France

³CNRS, UMR5223, Ingénierie des Matériaux Polymères, Villeurbanne, France

Received 26 June 2009; accepted 11 February 2010

DOI 10.1002/app.32405

Published online 15 July 2010 in Wiley InterScience (www.interscience.wiley.com).

ABSTRACT: This study provides information on the mechanical behavior of epoxy-poly(methyl methacrylate) (PMMA)-clay ternary composites, which have been prepared using the phase separation phenomenon of PMMA and the introduction of organophilic-modified montmorillonites (MMTs), the continuous matrix being the epoxy network. Two dispersion processing methods are used: a melt processing without any solvent and an ultrasonic technique with solvent and a high-speed stirrer. TEM analysis shows that phase separation between PMMA and the epoxy network was obtained in the shape of spherical nodules in the presence of the clay in both process methods used. Nanoclay particles were finely dispersed inside thermosetting matrix predominantly delaminated when ultrasonic blending was used; whereas micrometer-sized aggregates were formed when melt blending was used.

The mechanical behavior of the ternary nanocomposites was characterized using three-point bending test, dynamic mechanical analysis (DMA), and linear elastic fracture mechanics. The corresponding fracture surfaces were examined by scanning electron microscopy to identify the relevant fracture mechanisms involved. It was evidenced that the better dispersion does not give the highest toughness because ternary nanocomposites obtained by melt blending present the highest fracture parameters (K_{Ic}). Some remaining disordered clay tactoids seem necessary to promote some specific toughening mechanisms. © 2010 Wiley Periodicals, Inc. *J Appl Polym Sci* 118: 3632–3642, 2010

Key words: clay; nanocomposites; epoxy; PMMA; ternary blends; processing conditions; fracture

INTRODUCTION

The mechanical properties of epoxy-layered silicate nanocomposites have been widely studied, because these new modifiers are a real alternative of reinforcement compared with usual fillers.^{1,2} Layered silicates can compete both from an economic point of view and from the performances obtained with a very low amount of clay due to a dramatic aspect ratio.

Because of their mechanical and chemical properties, thermosetting (TS) polymers have increased their applications in composite materials for a wide range of automotive and aerospace applications.³ Epoxies are a kind of TS polymer used in these areas as adhesives in structural applications and in composite matrices because of their high stiffness and good heat and solvent resistance. Nevertheless, TS

materials are limited owing to their brittleness. Over the last 30 years, researchers have been trying to solve this problem using mixtures of TS resin with functionalized rubbers (like CTBN), preformed particles (like core shell), and thermoplastics (like poly(methyl methacrylate) (PMMA), PS, or PES, PEI) to increase the toughness.^{3,4}

At very low volume ratio of organoclay, nanocomposites generally exhibit significantly improved mechanical properties (stiffness, toughness, and their balance), but these mechanical properties are mainly dependent on filler size, organophilic treatment, and on intercalation/exfoliation dispersion state at the end of reaction.^{5–10} A wide range of research about the preparation and exfoliation mechanisms of epoxy-layered nanocomposites has been developed since the first works of Pinnavaia and Beall.⁶ Wang et al.¹¹ published a very interesting work on DGEBA/DETDA network. A good exfoliation state was obtained using a so-called “slurry compounding.” Such a process proved to be very efficient and better than conventional mixing. The state of dispersion is strongly influenced by the processing conditions and the reaction kinetics. Recently, a synergy was researched by preparing ternary systems based

Correspondence to: J. Duchet-Rumeau (jannick.duchet@insa-lyon.fr).

Contract grant sponsor: CONACYT (Mexico).

on clay, epoxy, and a third additive that can be miscible or not with epoxy precursor. Among nonmiscible additives, core shell rubber (CSR) particles are interesting additives to strengthen epoxy/clay nanocomposites.¹² In the case of initially miscible additives like rubber, thermoplastic or precursors for sol-gel chemistry, phase separation appears during reaction (reaction-induced phase separation, RIPS),³ leading to a ternary-phase system. In this case, the miscible additive could help the clay exfoliation acting as a processing aid. Many articles deal with rubber-modified epoxies with organophilic-layered silicates. Different rubbers were used: polyether rubbers,¹³ polyether polyols,¹⁴ carboxyl-terminated butadiene-acrylonitrile copolymers (CTBN),^{15,16} or hyperbranched polymers.¹⁷ In most cases, stiffness was the result of balancing the ratio of soft and hard fillers, and toughness was improved via multiple cracks and crack bifurcation mechanisms. Thermoplastics undergoing RIPS as PMMA were also used, leading to significant improvements in toughness.^{18,19} Not only rubbers but also TPs can have a toughening effect at room temperature, mainly by crack bridging and crack pinning mechanisms.^{3,4}

However, currently, there are not many studies that use the phenomenon of phase separation of a thermoplastic into an epoxy matrix in the presence of clay.¹⁹ In this context, the goal of this work is to achieve a ternary nanocomposite system, with a continuous epoxy matrix, using an initially miscible thermoplastic to obtain a separated phase and at the same time to disperse a clay using two different methods of dispersion, i.e., melt intercalation or ultrasonic processing. PMMA was chosen because of its solubility in the initial epoxy prepolymer, diglycidyl ether of bisphenol A (DGEBA) and because the phase separation was previously investigated in the binary blend epoxy/PMMA.²⁰ This study was done with an amount of PMMA below the critical volume fraction to keep a continuous epoxy matrix.

The originality and relevance of this work is based on the inclusion of a thermoplastic phase, PMMA initially miscible in the epoxy precursors, that can help the mechanism of dispersion of clay in the TS matrix during curing and phase separation steps and to promote its own toughening effect and possible interactive mechanisms. What kind of morphologies can be obtained by considering the dispersion processing methods, the molecular weight of PMMA, and the clay organophilic treatment? Figure 1 illustrates some possibilities for structuring the final composite: (a) thermoplastic and clay may remain separated and dispersed in the epoxy-amine matrix, (b) thermoplastic can separate inside the intercalated clay, (c) clay can be embedded into the PMMA separate phase, or (d) any other combination or coexistence of the three possibilities can be considered.

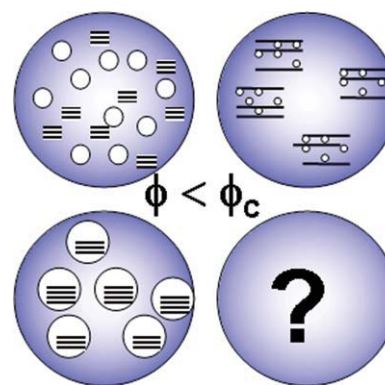


Figure 1 Different possible morphologies of a ternary nanocomposite. [Color figure can be viewed in the online issue, which is available at www.interscience.wiley.com.]

MATERIALS AND METHODS

Materials

The epoxy/montmorillonite (MMT)/PMMA nanocomposite was prepared using the epoxy prepolymer DGEBA with $\bar{m} = 0.15$ (LY556 from Vantico). The hardener chosen was the aromatic 4,4' methylene dianiline (MDA) with an analytical grade from Aldrich.²⁰ The thermoplastic polymer used was a poly(methylmethacrylate) (further noted PMMA-1) with an average molar mass 50,000 g mol⁻¹. A PMMA of low molecular weight, named PMMA-2, was synthesized in our laboratory. The polymerization of MMA was prepared by free radical polymerization in dried toluene.

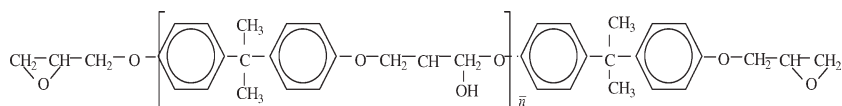
All the chemicals, MMA monomer, azobisisobutyronitrile (AIBN) initiator, 1-dodecanethiol (*n*-DDM) like transfer agent were purchased from Aldrich and were used as received besides MMA, which was distilled. The reactive mixture is made of 6.80 g of distilled MMA, 0.21 g of AIBN, 1.63 g of 1-dodecanethiol, and 15 cc of dried toluene. The polymerization is carried out at 80°C for 4 h under strong mechanical stirring (at 100 rpm) and nitrogen atmosphere. Then, the synthesized product was precipitated in cold heptane to recover the PMMA-2 that is dried in an oven at 60°C for 24 h. The molar mass determined by SEC was around 1100 g/mol with a polydispersity index of 2.

Two organophilic MMTs were used. The first one is the Cloisite 30B, modified by methyl, tallow, bis-2-hydroxyethyl quaternary ammonium chloride ions and supplied by Southern Clay Products (USA). Another organophilic modification was performed in the laboratory on sodic clay, Optigel EXO255 supplied from Süd Chemie (Germany). The cationic exchange, well described in another article,²¹ was carried out with the acryloxyethyl dimethylbenzylammonium chloride that is Adamquat BZ80 from Arkema. This surfactant is terminated with a

TABLE I
Characteristics of Components Used

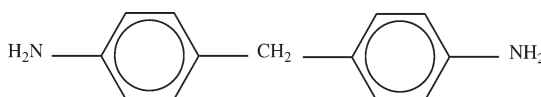
Supplier: Vantico
 Trade name: LY556
 Mass = 382.6 g mol⁻¹
 $\bar{n} = 0.15$

Diglycidyl ether of bisphenol A (DGEBA)



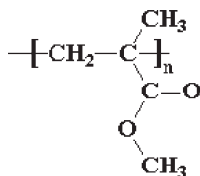
Supplier: Aldrich
 Mass = 198 g mol⁻¹

Methylene dianiline (MDA) (DGEBA)



Supplier: Arkema
 For PMMA-1: $\bar{M}_n = 43$ kg mol⁻¹
 and IP = 2.07
 For PMMA-2: $\bar{M}_n = 1$ kg mol⁻¹
 and IP = 1.97

Polymethyl methacrylate (PMMA) (DGEBA)



methacrylate function, which could increase the compatibility toward PMMA. The different characteristics and structures of materials are listed in Table I for polymers and in Table II for modified clays.

Processing

Two processing methods are used for preparing the ternary nanocomposites: melt and ultrasonic dispersion. The main difference is that THF was used as a solvent in the ultrasonic method.

Ultrasonic probe dispersion (with THF)

PMMA is first dissolved in a 10 wt % THF solution under a magnetic stirring at 40°C for 1 h, then the clay is added, and all the system is mixed using an ultrasonic probe (Vibracell 75022-130 Watts and 20 kHz) at room temperature for 30 min. An appropriate amount of DGEBA is introduced in the PMMA solution and mixed mechanically using a Rayneri turbostirrer at 2000 rpm at 135°C for 2 h. At this

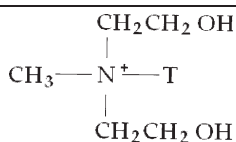
point, the solvent is evaporated, finally the amine is added, and the mixing is stopped after 5 min.

Melt dispersion (without solvent)

DGEBA and PMMA (1 or 2) are mixed in a glass reactor at 135°C, and after 2 h, a transparent and homogeneous solution is obtained. At this moment, the clay is added and is mixed with a Rayneri turbostirrer at 2000 rpm at 135°C for 2 h. Finally, the curing agent is introduced into the system and followed by 5 min of stirring. In both cases, the hardener is used with a stoichiometric ratio of epoxy to amino-hydrogen groups equal to 1, and an amount of 10 phr for whatever PMMA used and 5 phr for Cloisite30B are introduced. In this work, phr is used rather than wt % because the formulation could be modified without changing the amount of neat resin. To compare with other results in the literature, composites containing 10 phr of PMMA and 5 phr of MMT really contain ~ 9 wt % PMMA and 4.3 wt % of MMT, respectively. Keep in mind that modified MMT

TABLE II
Characteristics of Organophilic MMTs

Supplier: Southern Clay Pdts
 Trade name: Cloisite 30B
 Intergallery distance: 18 Å
 CEC = 90 mequiv/100 g



Supplier: Süd chemie for pristine MMT
 name: MMT-BZ80
 Intergallery distance: 17.7 Å
 CEC = 73 mequiv/100 g

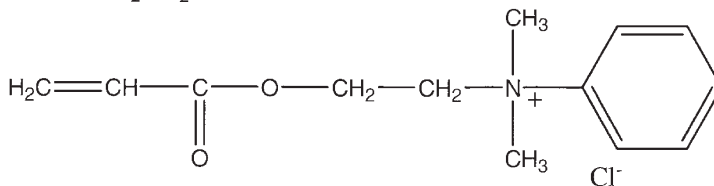


TABLE III
Description and Designation of Studied Ternary Nanocomposite Blends

Sample	Signification and Introduction technique
S ₁	Ternary blend: ultrasonic probe technique ([PMMA-1 + THF] (10 phr) + 30B(5 phr)] + DGEBA) + MDA -PMMA-1= 50,000 g mol ⁻¹ -Dispersion of clay in PMMA dissolved in THF with the ultrasonic probe for 1 h at room temperature. -Introduction of DGEBA within the mixture at 135°C -Time dispersion: 2 h at 135°C before adding the amine. -Curing cycle: 4 h at 135°C and 2 h at 200°C
S ₂	Ternary blend: melt technique [DGEBA + PMMA-1 (10 phr) +30B(5 phr)] + MDA - PMMA-1= 50,000 g mol ⁻¹ PMMA, clay, and DGEBA are mixed for 2 h at 135°C before adding the amine. -Curing cycle: 4 h at 135°C and 2 h at 200°C
S ₃	Ternary blend: melt technique [DGEBA + PMMA-2 (10 phr) +30B(5 phr)] + MDA - PMMA-2= 1000 g mol ⁻¹ (Same process as S ₂)
S ₄	Ternary blend: melt technique [DGEBA + PMMA-1 (10 phr) +BZ80(5 phr)] + MDA - PMMA-1= 50,000 g mol ⁻¹ (Same process as S ₂)

always shows more or less 30% of organic phase,²¹ so the amount of inorganic part is only ~ 3 wt %. After the amine dissolution step at 135°C, all the mixtures are submitted to a curing cycle including 4 h at 135°C and 2 h at 200°C in a metallic mold covered with PTFE sheets. Modeling of the kinetics of the reaction and the phase separation influence was previously done and corresponds with the experimental results.¹⁸

Designation of samples and their preparation are summarized in Table III.

Characterization

The clay dispersion in the ternary blends was characterized by wide angle X-ray scattering (WAXS) at the Henry Longchambon Diffractometry Center that measures the interlayer distances on a Siemens D500 with a copper anode, working with a 20 kV tension and 30 mA intensity. Transmission electron microscopy (TEM) was performed at the Technical Center of Microstructures on a Phillips CM 120 microscope operating at 80 kV to characterize the morphology of ternary blends. Samples have been prepared using an ultramicrotome at room temperature. Phase separation was also checked on cured samples using DMA, performed on a Rheometric Solid Analyzer (RSA II), working in a temperature range between 50 and 250°C and with a frequency of 1 Hz to obtain storage modulus G' , loss modulus G'' , and loss factor $\tan \delta$ between 50 and 250°C. Samples were parallelepipedic bars (1.5 × 2.5 × 25 mm³). Young's modulus

and Poisson ratio are obtained on the ISO 60 specimen with crossed strain gauges (from Vishay Micro-measure), in tension, at a speed of 1 mm/min, on a 2/M MTS set up at a constant temperature of 22°C. The accuracy on the moduli is estimated at 0.1 GPa. Mode-I critical stress intensity factor (K_{Ic}) was determined in SEN geometry at a speed of 10 mm/min according to ESIS protocol,²² and the values are given with an accuracy of 0.05 MPa m^{1/2}. G_{Ic} could be easily calculated but is not discussed in this work because the elastic constants of the materials under study are roughly the same. The fracture mechanisms were analyzed by scanning electron microscopy (SEM) on a Phillips XL20 microscope working with a tension of acceleration between 5 and 10 KV.

RESULTS AND DISCUSSION

Influence of processing method

Morphology of thermoplastic/thermosetting blend

The blends based on PMMA and DGEBA are miscible whatever the mixture composition is. The DMA performed on thermoplastic/TS blend ($\tan \delta$ and G' evolution versus temperature) shown in Figure 2 highlights the phase separation appeared during reaction with MDA amine as both relaxation peaks visualized, $T_{\alpha 1}$ with a maximum around 175°C and $T_{\alpha 2}$, with a maximum around 120°C, can be clearly associated to the relaxation of epoxy-amine network ($T_{\alpha} = 173^\circ\text{C}$) and PMMA ($T_{\alpha} = 128^\circ\text{C}$), respectively. The decrease of the relaxation temperature related to PMMA can be explained by a small amount of DGEBA monomer remained dissolved into PMMA. Figure 3 reveals the presence of PMMA in the shape of small white nodules, resulting from the phase separation during curing of the epoxy-amine network.²⁰ The diameter of these PMMA particles

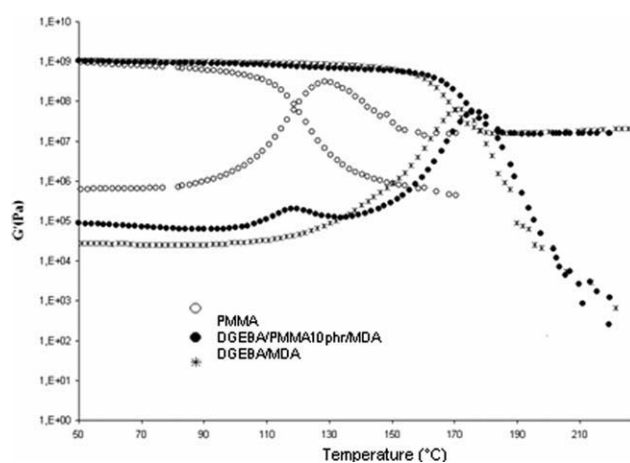


Figure 2 Dynamic mechanical spectra (at a frequency of 1 Hz) performed on neat materials PMMA and epoxy-amine system and on PMMA-10 phr/DGEBA-MDA blend.

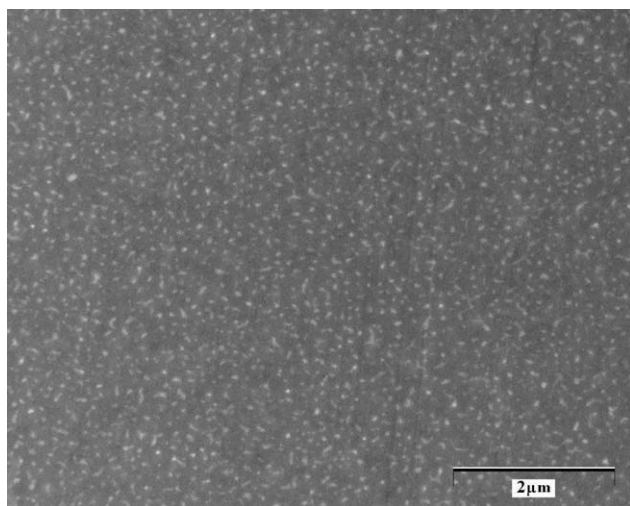


Figure 3 TEM image performed on the DGEBA-MDA/PMMA-10 phr blend.

homogeneously distributed in the matrix ranges between 30 and 70 nm. The introduction of small PMMA particles showing the same stiffness as epoxy-amine matrix makes increase the network relaxation temperature about a few degrees.

Morphology of cured ternary blends

Wide angle X-ray spectra performed on ternary blends obtained by ultrasonic probe (S_1) and by melt process (S_2), respectively, are presented in Figure 4. Each spectrum is compared to the Cloisite 30B one, which shows clearly a well-defined peak at $2\theta = 5^\circ$, assigned to the initial interlayer spacing $d_{001} = 1.79$ nm and characteristic of the clay crystalline structure. None of the spectra realized on the ternary nanocomposites exhibits a diffraction peak, which highlights the lack of repeated structures of equal spacing in the distance range investigated. However, we cannot speak of exfoliation because the lack of Bragg scattering may only indicate that the distances between two consecutive platelets are too great to be detected (higher than 80 \AA , which is the limit distance to be detected by WAXS). We are only sure that monomers and increasing polymer chains have diffused into clay galleries and opened them. The X-ray spectrum performed on the ternary blends processed using the ultrasonic probe technique (S_1) shows a different evolution in the small angle window, next to the direct beam. A correlation peak appears unlike other nanocomposites. The TEM characterization reported in Figure 5 identifies the different morphologies of the composite S_1 obtained by the ultrasonic probe technique. In Figure 5(a), the clay with a structure of small tactoids is homogeneously distributed and randomly dispersed throughout the matrix. The TEM image at higher magnifica-

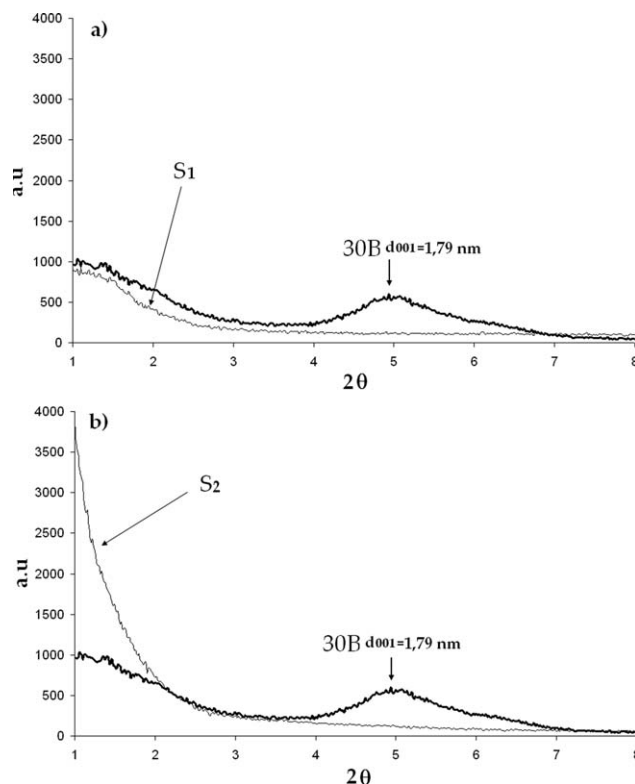


Figure 4 X-ray diffraction spectra of the cured samples: (a) S_1 and (b) S_2 . Both of them are compared with the Cloisite 30B clay spectrum.

tion reported in Figure 5(b) shows that the tactoids present average interlayer distances of around 22 nm. TEM images performed on nanocomposites obtained by melt process (S_2) are reported in Figure 6. At low magnification [Fig. 6(a)], we observe the presence of small tactoids that coexist with large aggregates of silicate within the matrix. The distance of separation between them is about $10 \mu\text{m}$, and the size of the aggregates varies from 1 to $5 \mu\text{m}$. In the same way, at higher magnification [Fig. 6(b)], the small white nodules of PMMA form a separate phase with an average diameter of 70 nm, showing the presence of clay does not disturb the phase separation during curing of the epoxy-amine network.

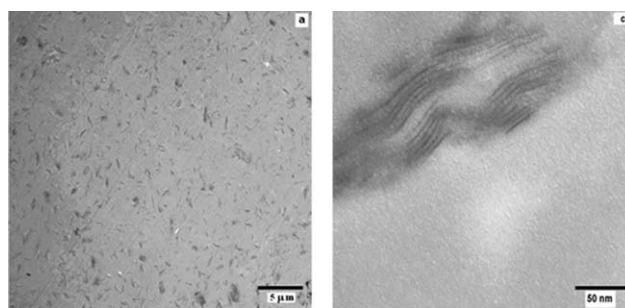


Figure 5 TEM images of S_1 cured nanocomposites performed with solvent and an ultrasonic probe coupled with a high-speed disperser: (a) general view and (b) evidence of the separation of silicate monolayers.

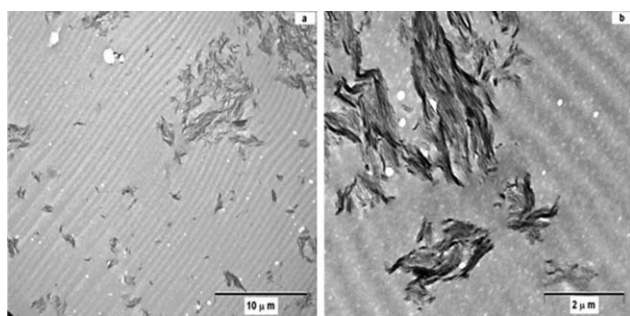


Figure 6 TEM images of S_2 cured nanocomposites without solvent and performed with melt dispersion: (a) general view, (b) agglomerates and evidence of the phase separation of PMMA-1.

At first view, the use of solvent and ultrasonic probe is a more efficient way to obtain a homogeneous dispersion of small tactoids than the melt process, which leads to a considerable amount of clusters of much larger size. In both cases, the PMMA phase separation takes place. It seems that clays are only contained in the epoxy continuous phase and are not observed inside PMMA nodules. Furthermore, the presence of clay does not modify the morphology of the PMMA phase in the TS network. TEM micrographs thus suggest that the best dispersion of small primary particles is obtained when the ultrasonic probe technique is used. Yet, we must keep in mind that TEM is a local analytical technique, and the distances measured on the micrographs are not really significant of the whole sample.

SAXS analysis was carried out before and allowed to complete the insight into the mechanism of dispersion and into the relative efficiency of the systems of dispersion used.²³ The exfoliation state of the silicate layers in blends synthesized using both methods has been investigated on the cured systems and during the curing reaction. The attention was focused on the distribution of thicknesses of the diffusing particles. SAXS analysis has shown that exfoliation of the platelets can occur through the deaggregation of large agglomerates into particles composed of a few platelets. At the end of the process, the filler is well dispersed as single sheets. SAXS *in situ* study made on samples obtained by ultrasonic probe dispersion shows that final morphology is more homogeneously exfoliated, and correla-

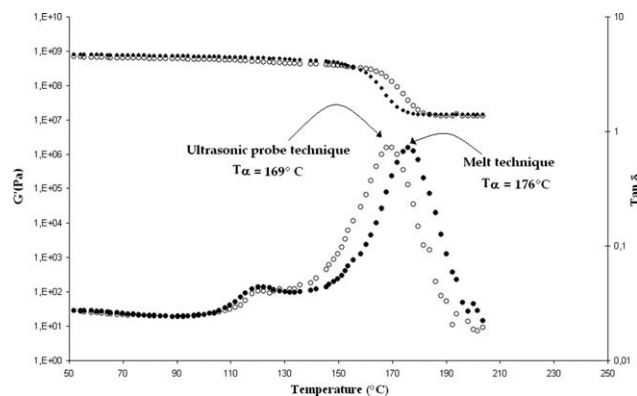


Figure 7 Dynamic mechanical spectra (at a frequency of 1 Hz) performed on S_1 samples processed with ultrasonic probe and on S_2 samples processed with melt process.

tions cannot be neglected between the exfoliated sheets, whereas for the sample obtained by melt dispersion, large size agglomerates are present with single platelets and no correlation peak is observed. These three analysis techniques, WAXS, TEM, and SAXS, are really complementary because they cover several observation scales and allow a complete insight into nanocomposite morphology.

DMA ($\tan \delta$ and G' evolution versus temperature) is shown in Figure 7, whereas the values of softening mechanical transition temperature $T_{\alpha 1}$ (associated to the glass transition temperature of the epoxy network) and storage modulus (G') obtained for all reference systems and for both ternary systems (S_1) and (S_2) are reported in Table IV. We can see that the use of solvent has a little consequence on the position of $T_{\alpha 1}$ as a decrease of almost 10°C is measured. This could be attributed to remaining solvent and/or more dissolved PMMA in the epoxy phase. The PMMA phase separation is confirmed by the dynamic analysis as a second relaxation peak, $T_{\alpha 2}$, with a maximum around 120°C , close to the relaxation of pure PMMA is observed independently of the dispersion technique.

In conclusion, the studies by SAXS, TEM, and WAXS show that ultrasonic probe processing induced a better dispersion of clay at every scale, in comparison with the methodology of the melt process. In both cases, the PMMA phase separation was not affected.

TABLE IV
Dynamic Mechanical Analysis Values Obtained for Reference Systems and for Both Ternary Composites S_1 and S_2

	DGEBA/ MDA	PMMA	DGEBA/ MDA-PMMA-1 (10 phr)	DGEBA/ 30B/MDA	S_1	S_2
$T_{\alpha 1}$ ($^\circ\text{C}$)	173		175	178	169	176
G'_{T_m+50} (MPa)	13		10	19	12	12
$T_{\alpha 2}$ ($^\circ\text{C}$)		128 $^\circ\text{C}$	118		120	121

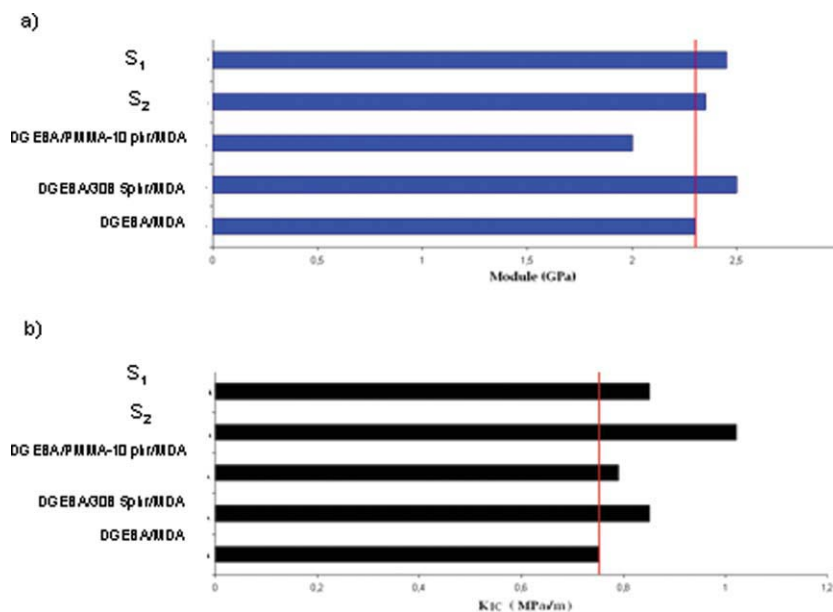


Figure 8 Mechanical characteristics at 25°C of S₁ and S₂ ternary composites compared with the pure thermosetting matrix and binary blends with clay or with PMMA: (a) modulus and (b) critical stress intensity factor (K_{IC}). [Color figure can be viewed in the online issue, which is available at www.interscience.wiley.com.]

Next, the consequences of these different dispersion methods on mechanical properties were investigated.

Mechanical properties of cured ternary blends

Two main mechanical properties will be now discussed: stiffness by comparison of Young's modulus and toughness using K_{IC} values. Figure 8(a,b) illustrates the values of the modulus and the critical stress intensity factor (K_{IC}), respectively, for the different systems: pure epoxy-amine matrix, filled with clay alone, blended with thermoplastic phase alone and ternary blends (S₁) and (S₂) samples obtained from the two processing methods previously described.

By comparison to neat epoxy-amine network, the incorporation of 5 phr of clay increases both the stiffness as modulus increases from 2.3 to 2.5 GPa and the toughness as K_{IC} has a little increase from 0.75 to 0.85 MPa m^{1/2}. The effect of nanofillers on the improvement of compromise "stiffness–toughness" is the characteristic of nanocomposites. This reinforcement is attributed to the increase of crack path due to the tortuosity created by platelet fillers. On the other side, 10 phr of PMMA introduced in TS matrix leads to a decrease of modulus from 2.3 to 2.0 GPa; meanwhile, a slight increase of K_{IC} (from 0.75 to 0.79 MPa m^{1/2}) is observed. The mechanism of cavitation induced by separated PMMA particles can explain this increase of toughness but also the crack pinning and crack bridging mechanisms, which are the most often promoted by TP particles.

For ternary systems, when the both additives are present, a synergy occurs as the resistance to crack

propagation is enhanced without significant loss of modulus. A similar effect was exhibited by Lee et al. on epoxy/MMT/CTBN ternary blends, where the impact strength evidenced a maximum and is multiplied by 2 by adding 2% MMT. The addition of both PMMA and clay in the epoxy-amine matrix increases the modulus of each system, from 2.30 (for pure epoxy-amine matrix) to 2.35 GPa for ternary system (S₂) and to 2.45 GPa for ternary system (S₁). These results show the benefit of adding clay, in small amounts (about 3 wt % of pure inorganic filler) to balance the modulus decrease caused by PMMA. This effect was also observed on an epoxy-rubber-clay system^{16,24} and ternary blends epoxy/clay/hyperbranched polymers.²⁵ The toughness of the ternary composite realized by the melt process increases from 0.75 to 1.02 MPa m^{1/2}, whereas for the ternary composite achieved by ultrasonic probe, the value increases from 0.75 to 0.85 MPa m^{1/2} only. Therefore, it was obtained for the ternary composite elaborated by the melt process a 36% increase in toughness compared with a 13% increase for the sample obtained by ultrasonic probe technique. However, these increases remain more significant than for binary systems where PMMA phase is added without fillers.

The preconceived and often advanced idea in the literature that the complete exfoliation of clay is the morphology required to improve the mechanical properties of composites is not verified experimentally in this work. Here, we could expect that a homogenous distribution at all scales of primary particles in the nanocomposite obtained by ultrasonic

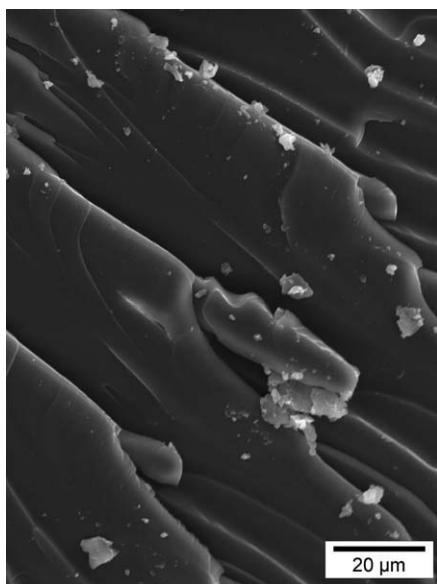


Figure 9 SEM image on fractured surface of the neat epoxy matrix (DGEBA/MDA).

probe and solvent would allow a good stiffness/toughness compromise.^{11,24} However, the best result achieved in toughness (increase of 36%) was obtained on the nanocomposites synthesized by the melt process, where the structure is more heterogeneous with small tactoids coexisting with larger aggregates. The multistructural morphology seems to be more effective to increase the dissipated energy during fracture. The presence of aggregates does not appear to be harmful and can even modify and increase the path of crack propagation.²⁴ Not too large agglomerates, well structured, can improve the crack propagation resistance, via decohesion at the interfaces, thus increasing the energy consumed. The occluded volume in the aggregates could also explain the toughness increase via un volume fraction effect.

To understand the influence of both clay and thermoplastic on the behavior of fracture, an analysis by SEM was carried out. Figure 9 shows the fractured surface of the pure matrix (DGEBA/MDA), which is characteristic of a brittle material. Figure 10(a,b) shows the micrographs performed on fractured surfaces of ternary composites processed either by the ultrasonic probe technique or melt process, respectively. At the same magnification, these images reveal different crack paths depending on processing way. For the ternary system synthesized by the melt process, these cracks are many and very branched, whereas for the ternary composite obtained by ultrasonic probe, the fractured surface is less tortuous. The presence of junctions and ramifications is seen as a means of energy dissipation.^{10,24,26,27} Figure 11(a,b) reports micrographs corresponding to the same ternary composites but with a higher magnification. The very different roughness

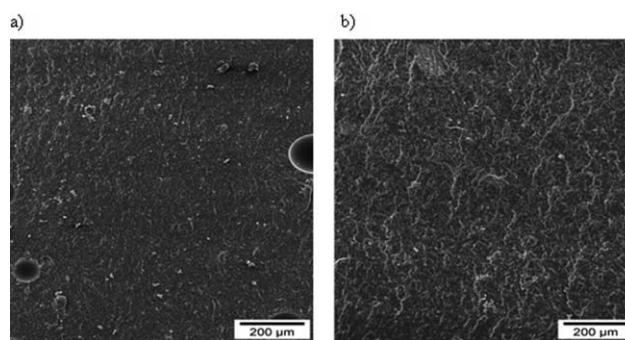


Figure 10 SEM image on fractured surface of ternary composites synthesized by: (a) ultrasonic probe technique (S_1) and (b) melt process (S_2).

between these two materials explains the differences of morphology observed. The presence of clay makes the crack follow more tortuous paths due to possible crack deflection mechanism.^{11,25} It is possible that for the composite obtained by the melt process, the polymerization is not homogeneous and that the curing inside the layers of clay could be different from the one performed outside of them, so it is possible that the formation of induced internal stresses contributes to reduce the crack propagation resistance.²⁶

Influence of molecular weight of PMMA

To facilitate the clay dispersion into thermoplastic phase, we have synthesized a PMMA with a low molecular weight (1000 g/mol), which should help its diffusion between clay layers. These ternary blends are elaborated only by melt process with 10 phr of PMMA-2 and 5 phr of Cloisite 30B.

On PMMA/epoxy binary blends

The DMA reported in Figure 12 and realized on a postcured binary blend shows a single relaxation peak situated at a maximum temperature about 157°C. With a lower molecular weight PMMA, the

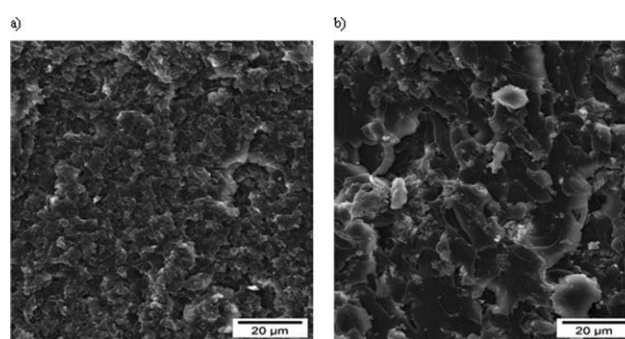


Figure 11 SEM images at highest magnification performed on fractured surfaces of ternary composites synthesized by: (a) ultrasonic probe technique (S_1) and (b) melt process (S_2).

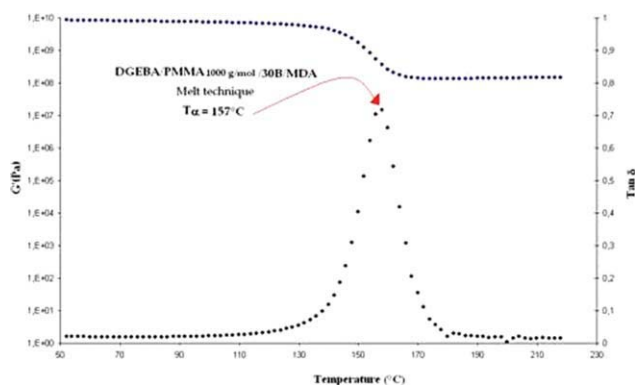


Figure 12 Dynamic mechanical spectra (at a frequency of 1 Hz) for a ternary composite obtained with a PMMA of 1000 g mol^{-1} (10 phr) and Cloisite 30B (5 phr) by melt process. [Color figure can be viewed in the online issue, which is available at www.interscience.wiley.com.]

phase separation was not detected by TEM and DMA. The relaxation maximum temperature is strongly decreased of almost 20°C in comparison with PMMA-1 of $50,000 \text{ g/mol}$ (in this last case, T_α is about 175°C). The low molecular weight of thermoplastic is the cause of this decrease of relaxation temperature, as the T_g of PMMA-2 of 1000 g/mol has a value of 25°C . Using Fox's equation and assuming a full miscibility of the PMMA-2, the relaxation of this homogeneous matrix would be around 150°C , which is not too far away from 157°C .

On ternary blend mechanical properties

The mechanical behavior of this ternary blend realized with the low-molecular-weight PMMA is reported in Figure 13 and is compared with the ternary blend prepared with the higher molecular weight PMMA. The modulus of ternary composite with low-molecular-weight PMMA-2 remains

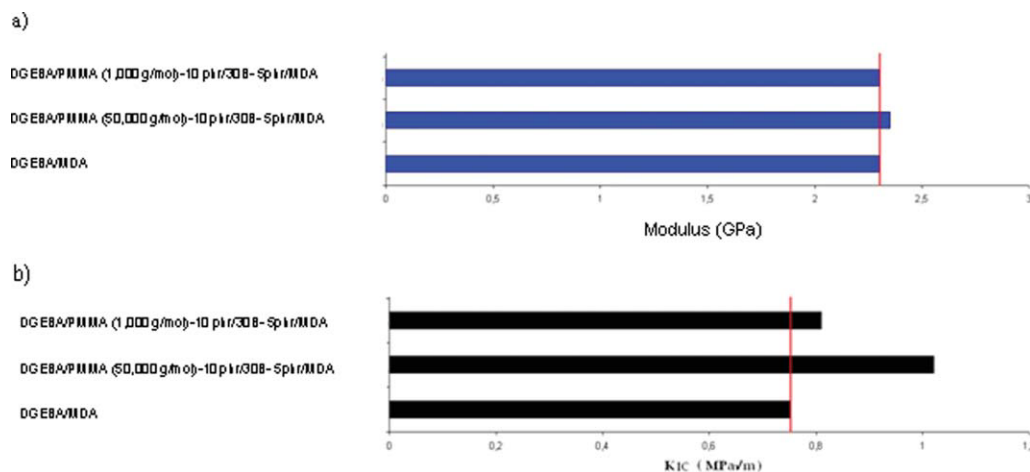


Figure 13 Effect of PMMA molecular weight on mechanical characteristics at 25°C compared with the pure matrix: (a) modulus and (b) critical stress intensity factor (K_{Ic}). [Color figure can be viewed in the online issue, which is available at www.interscience.wiley.com.]

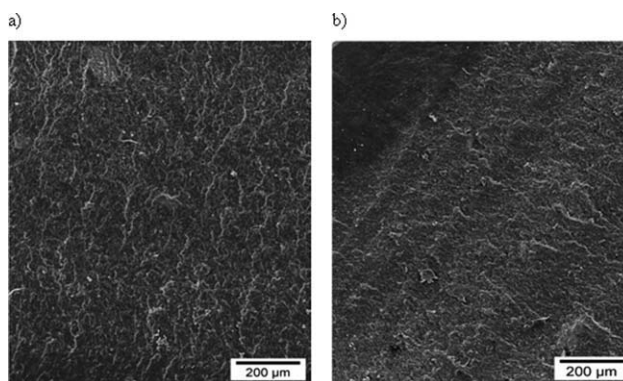


Figure 14 SEM images performed on fractured surfaces of ternary composites: (a) (S_2) and (b) (S_3).

unchanged in comparison with the epoxy-amine matrix as shown in Figure 13(a). A slightly higher modulus is measured when high-molecular-weight PMMA is used. Concerning the critical stress intensity factor (K_{Ic}) reported in Figure 13(b), the increase of K_{Ic} is low (only a gain of 8%) respective to pure matrix and to samples prepared with a higher molecular weight PMMA (increase of 36%). The low molecular weight of PMMA is not conducive to improve the mechanical properties because of its total miscibility and proves that phase separation is compulsory for toughness improvement.^{3,4} SEM images performed on fractured surfaces of ternary composites and shown in Figure 14 illustrate the fracture mechanisms implied. The crack paths are not branched enough for increasing the fracture energy unlike to higher molecular weight PMMA.

Influence of organophilic treatment of clay

To modulate physicochemical interactions between nanoclay and thermoplastic/TS blend, a new surfactant based on methacrylate-functionalized quaternary

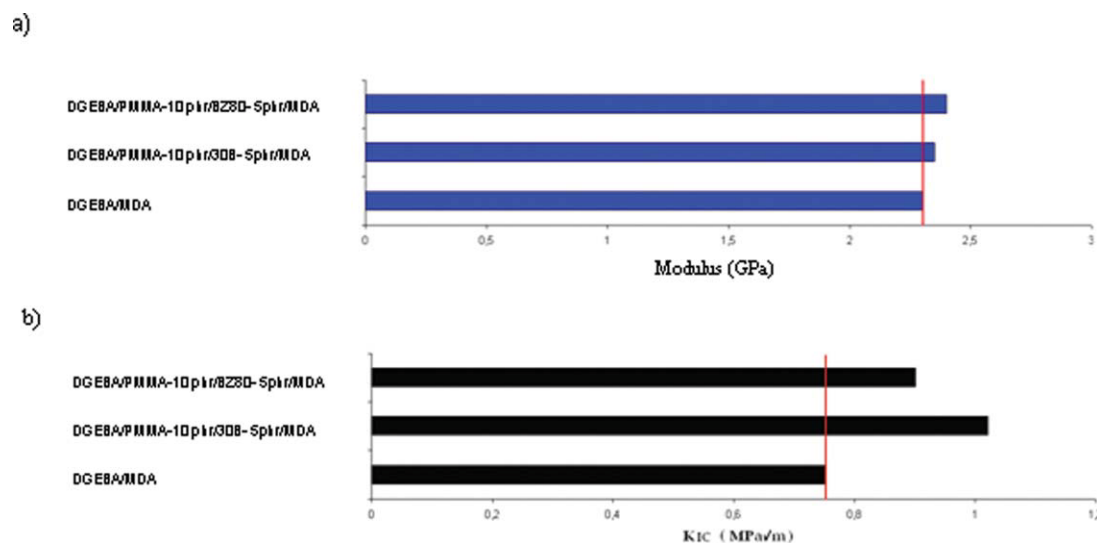


Figure 15 Effect of clay surface treatment on mechanical characteristics at 25°C compared with the pure matrix: (a) modulus and (b) critical stress intensity factor (K_{Ic}). [Color figure can be viewed in the online issue, which is available at www.interscience.wiley.com.]

ammonium was used. Compared with ammonium ions used in Cloisite 30B showing a hydrophobic/hydrophilic balance divided between alkyl chains and alcohol groups, acryloxyethyl dimethyl benzyl ammonium ion owns a reactive function through the vinylic double bond that may react with MMA monomer during *in situ* polymerization²⁸ and improves the miscibility with PMMA chains. This new modified clay was introduced into the binary blend based on high-molecular-weight PMMA and epoxy-amine system prepared by melt way. The mechanical analysis summarized in Figure 15 reveals that the clay modified by methacrylate groups leads to a slightly higher modulus than the one obtained with Cloisite 30B as an increase of 4.3% against 2.2% for Cloisite 30B was obtained as shown in Figure 15(a). Matrix toughness was also increased respect to pure TS matrix one. However, this increase remains lower than the one obtained with Cloisite 30B (20% against 36%).

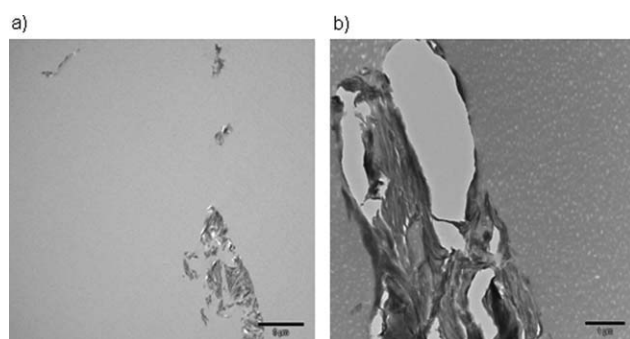


Figure 16 Effect of clay surface treatment on ternary system morphology determined by TEM analysis: (a) DGEBA-MDA/PMMA-1/clay 30B and (b) DGEBA-MDA/PMMA-1/clay BZ80.

The expected miscibility between methacrylate-functionalized clay and thermoplastic/TS blends does not seem to play an effective role. The morphology of resulting materials is very disappointing as large aggregates with a size varying between 4 and 13 μm are detected by TEM as shown in Figure 16. The phase separation phenomenon always takes place but without interaction with clays. The presence of aggregates reduces the chain mobility increasing the glass temperature (181°C with BZ80 against 176°C with Cloisite 30B). This increase of T_g can be attributed not only to the presence of aggregates and possible occluded volume but also to a lower miscibility of PMMA in the matrix. On fractured surfaces reported in Figure 17, large aggregates of BZ80 clay are also present. The crack trajectories in these composites show that the interaction of the crack with the clay is low as the paths are almost straight without branching. We can conclude that the conditions of dispersion used (time, speed, and temperature) are probably not sufficient to successfully disperse the clay modified with a much less efficient surfactant, i.e., BZ80. Some studies¹⁹ propose the existence of strong cohesive forces between the PMMA chains and attractive forces between the clay particles making the interface PMMA-clay low, which helps the spread of the crack propagation in the composites. The lower fracture energy could also be explained by the increase in T_g which usually decreases the toughness.

CONCLUSIONS

The objective of this work was to develop an epoxy-amine/MMT/PMMA ternary nanocomposite and to study the influence of processing conditions and

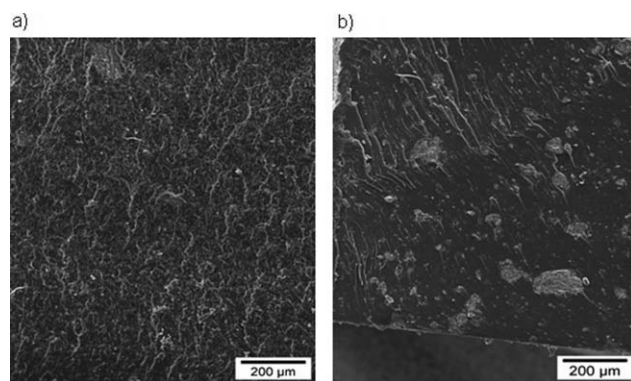


Figure 17 SEM pictures on fractured surfaces of ternary composites: (a) DGEBA-MDA/PMMA-1/clay 30B and (b) DGEBA-MDA/PMMA-1/clay BZ80.

clay surface treatment on mechanical properties. Two different processes of clay dispersion in the mixture of precursors were used: a melt and ultrasonic probe techniques. In both cases, the phase separation of PMMA composed of small nodules dispersed regularly in the matrix was highlighted. Using both these dispersion techniques, the clay was dispersed and reduced to the scale of tactoids, more homogeneously dispersed when the ultrasonic probe technique was used, as tactoids containing three or five sheets are observed in the system, whereas in the ternary composite obtained by melt processing, large size agglomerates are observed. Studies using linear elastic fracture mechanics have shown that the ternary composite obtained by the melt process has the highest fracture parameters (K_{Ic}) in comparison with the ternary system obtained by ultrasonic probe process. The influence of molecular weight of PMMA for obtaining a ternary composite was shown using a thermoplastic type PMMA of 1000 g/mol. This kind of PMMA is not optimized for obtaining a phase separation when it is introduced into the epoxy/clay/MDA system and the system did not exhibit any phase separation. Therefore, the low T_g of this polymer leads to a decrease of T_g of the final product. The ternary system obtained using the modified BZ80 clay does not further improve the mechanical properties of the system. The functionalization with the methacrylate group does not seem to be enough to improve the affinity with the PMMA matrix. Both the ethyl alcohol groups carried on Cloisite 30B are more efficient to induce an intimate contact with the matrix and improve the dispersion state.

In this work, the optimized conditions for obtaining a ternary composite with high fracture values were found: aggregates are more efficient than an exfoliation. A PMMA of 50,000 g mol⁻¹ helps to increase the fracture toughness, and finally the best dispersion process does not lead to the best mechan-

ical properties, and it seems that aggregates play a significant role in improving the resistance to crack propagation.

The authors thank Pierre Alcouffe and the Technical Center of Microstructures for providing the TEM characterization, Ruben Vera for performing the XRD experiments, and W.D. Cook for fruitful discussions.

References

1. Becker, O.; Simon, G. *Adv Polym Sci* 2005, 179, 29.
2. Wang, Z.; Massam, J.; Pinnavaia, T. J. In *Polymer Clay Nanocomposites*; Pinnavaia, T. J., Beall, G. W., Eds.; England: Wiley, 2000; p 127.
3. Pascault, J. P.; Sautereau, H.; Verdu, J.; Williams, R. J. J. *Thermosetting Polymers*; Marcel Dekker: New York, 2002; p 477.
4. Arends, C. B. *Polymer Toughening*; Marcel Dekker: New York, 1996; p 253.
5. Lan, T.; Kaviratna, P. D.; Pinnavaia, T. J. *Chem Mater* 1995, 7, 2144.
6. Pinnavaia, T. J.; Beall, G. W. *Polymer-Clay Nanocomposite*; Wiley: New York, 2000; p 343.
7. Kormann, X.; Thomann, R.; Mulhaupt, R.; Finter, J.; Berglund, L. *J Appl Polym Sci* 2002, 86, 2643.
8. Le Pluart, L.; Duchet, J.; Sautereau, H. *Polymer* 2005, 46, 12267.
9. Becker, O.; Simon, G. *Polymer Nanocomposites*; Woodhead Publishing Limited: Cambridge, 2006; p 29.
10. Zerda, A. S.; Lesser, A. J. *J Polym Sci Part B: Polym Phys* 2001, 39, 1137.
11. Wang, K.; Chen, L.; Wu, J.; Toh, M.; He, C.; Yee, A. *Macromolecules* 2005, 38, 788.
12. Gam, K. T.; Miyamoto, M.; Nishimura, R.; Sue, H. *J Polym Eng Sci* 2003, 43, 1635.
13. Frolich, J.; Thomann, R.; Mulhaupt, R. *Macromolecules* 2003, 36, 7205.
14. Isik, I.; Yilmazer, U.; Bayram, G. *Polymer* 2003, 44, 6371.
15. Liu, W.; Hoa, S. V.; Pugh, M. *Polym Eng Sci* 2004, 44, 1178.
16. Lee, H. B.; Kim, H. G.; Yoon, K. B.; Lee, D. H.; Min, K. E. *J Appl Polym Sci* 2009, 113, 685.
17. Becker, O.; Sopade, P.; Bourdonnay, R.; Halley, P. J.; Simon, G. *Polym Eng Sci* 2003, 43, 1683.
18. Hernandez, M.; Dupuy, J.; Duchet-Rumeau, J.; Sautereau, H. *e-Polymer* 2007, 102, 1.
19. Park, J. H.; Jana, S. C. *Polymer* 2003, 44, 2091.
20. Ritzenthaler, S.; Girard-Reydet, E.; Pascault, J. P. *Polymer* 2000, 41, 6375.
21. Lepluart, L.; Duchet, J.; Sautereau, H.; Gerard, J. F. *J Adhes* 2002, 78, 645.
22. Moore, D.; Pavan, A.; Williams, J. G. *Fracture Mechanics Testing Methods for Polymers, Adhesives and Composites*; ESIS Publication. Elsevier: Amsterdam, 2001.
23. Hernandez, M.; Sixou, B.; Duchet-Rumeau, J.; Sautereau, H. *Polymer* 2007, 48, 4075.
24. Balakrishnan, S.; Sart, P. R.; Raghavan, D.; Hudson, S. D. *Polymer* 2005, 46, 11255.
25. Becker, O.; Varley, R.; Simon, G. *Polymer* 2002, 43, 4365.
26. Zilg, C.; Mulhaupt, R.; Finter, J. *Macromol Chem Phys* 1999, 200, 661.
27. Miyagawa, H.; Misra, M.; Laurence, T. D.; Amar, K. M. *J Polym Environ* 2005, 13, 87.
28. Zeng, C.; Han, X.; Lee, J. L.; Koelling, K. W.; Tomasko, D. L. *Adv Mater* 2003, 15, 1743.